International Journal of Environmental Sciences
ISSN: 2229-7359
Vol. 11 No. 8, 2025
https://theaspd.com/index.php

Sustainable Machining of Titanium Alloy Ti-6Al-4V: Experimental Analysis Using Esterified Green Fluids

Cherian Paul[1], Rittin Abraham Kurien[2*], Steffan Mathew Cherian[3]
[1,2,3]Department of Mechanical Engineering, Saintgits College of Engineering (Autonomous), Kottayam, Kerala, 686532, India
Corresponding author*: Rittin Abraham Kurien (rittuak@gmail.com)

Abstract
Ti-6Al-4V titanium alloy is widely employed in aerospace, biomedical, defence, automotive, and cryogenic applications due to its superior strength-to-weight ratio, high-temperature stability, and corrosion resistance. Despite these advantages, its machining remains highly challenging, primarily attributed to low thermal conductivity, strong chemical reactivity with cutting tools, and inherent hardness. These characteristics lead to significant heat accumulation at the cutting interface, formation of segmented chips, dynamic cutting forces, accelerated tool wear, and compromised dimensional accuracy. To address these persistent issues, this study proposes the formulation of an eco-friendly, biodegradable cutting fluid derived from esterified Rubber Seed Oil, further enhanced with nano-additive, Molybdenum Disulphide. The proposed cutting fluid is designed to provide superior lubrication, efficient heat dissipation, and reduced friction during machining operations. A comprehensive experimental investigation will be conducted to evaluate the fluid's performance in lowering cutting temperatures, decreasing cutting forces, and improving surface integrity across varying cutting parameters. Additionally, the study examines its effectiveness in mitigating built-up edge formation and reducing material adhesion on the tool rake face. It is anticipated that the novel green cutting fluid will extend tool life, enhance process stability, and contribute to reduced energy consumption, thereby advancing sustainable manufacturing practices. Overall, the findings are expected to deliver valuable insights into enhancing the machinability of titanium alloys while addressing environmental and performance considerations.
Keywords: Machining; Biodegradable; Titanium alloy; Nano particles; Tool Wear

1. INTRODUCTION

In recent decades, the utilization of titanium alloys has significantly expanded across various high-performance sectors. Its strong strength-to-weight ratio, higher-temperature stability, and resisting corrosion make Ti-6Al-4V stand ahead [1]. However, machining of titanium alloys, particularly Ti-6Al-4V, presents considerable challenges. These arise primarily from its high hardness, strong chemical affinity with cutting tool materials leading to adhesion and diffusion wear and poor thermal conductivity, which results in excessive heat concentration in the cutting zone. These factors collectively contribute to accelerated tool wear, poor surface integrity, and increased energy consumption. Cutting parameters, especially cutting speed and feed rate, play a critical role in influencing both tool life and the resultant surface finish [2]. Therefore good lubricating oil that can reduce cutting temperature is to be used. But now a days the lubricating oil that we use are from non- renewable resources and are mostly no1 eco-friendly of which some are non-bio-degradable [3]. Therefore, the coolants that use must be capable of reducing the cutting temperature and maximize lubrication performance. Moreover it should be eco-friendly as most of the life style are based on sustainability and waste management [4]. Some of the key functions of the cutting fluids are to reduce the heat (to cool) and to lubricate the interface between the work piece and tool. Also to wash away the chips from machining surface that helps to reduce friction. Cutting fluid often contains oil from minerals, corrosive inhibitor, the fluorescein emulsifier and stabiliser. When we use excess of these elements it results in environmental impacts and wilt be hazardous to humans [5]. To mitigate the adverse effects associated with conventional cutting fluids, extensive research has been directed toward the development of alternative coolant solutions. These include the use of bio-based fluids derived from animal and vegetable oils, cryogenic cooling with liquid nitrogen, and the incorporation of nano-additives into various base fluids [6]. Li D. et al. [7] found that using an air-CO_2 combination to feed coolant particles to the tools-chip interface can significantly minimise tool wear in alloyed titanium machining. Additionally, the introduction of nanoparticles in moderate concentrations has shown potential in enhancing lubrication and thermal management at the cutting zone. Jordan M.I. et al. [8] explored sustainable cutting fluid strategies for machining Ti-6Al-4V using a life cycle assessment framework. Their findings revealed that tool life was reduced by approximately 75% under Minimum Quantity Lubrication (MQL) conditions (lasting less than 5 minutes) compared to both

flood cooling and cryogenic machining using LCO_2, where tool wear remained below 0.11 mm even after 20 minutes of machining. MQL was tested on Ti-6Al-4V machining using micro-hole patterned PCD & PCBN cutting elements by Paul C. et al. [9]. High feed rates increased flank wear, roughness at the surface, cutting temperature, and vibration, according to their research. However, customised PCD inserts under MQL circumstances excelled normal inserts in all metrics, rendering them an acceptable titanium alloy machining solution. Salvati E. et al. [10] assessed the machinability of Selective Laser Melted (SLM) Ti-6Al-4V parts. It was observed that the surface finish of machined SLM components was superior to conventionally produced parts. Despite the altered microstructure, increased hardness, and residual stresses inherent to the SLM process, machining behaviour remained comparable, thereby validating the applicability of conventional machining parameters for SLM-processed Ti-6Al-4V components. Wang H.J. et al. [11] studied the mechanical characteristics and microstructural evolution of CMT-added Ti–6Al–4V walls containing trace $MoSi_2$. The inclusion of $MoSi_2$ was found to enhance average strain capacity while reducing anisotropy in the fabricated parts. Fractographic analysis revealed dimpled surfaces, indicative of a ductile fracture mechanism. Chen J. et al. [12] examined textured cutting tool wear with Ti-6Al-4V machining using graphene-assisted MQL settings. Their results demonstrated improved tribological performance due to the reduced chip-tool contact on the rake face. Notably, tool life significantly increased with the use of surface-textured tools in combination with advanced lubrication environments. Zhan Z.X. et al. [13] emphasized the growing interest in additive manufacturing (AM) for producing components with complex geometries and customized material properties. In their study, Ti–6Al–4V alloy was fabricated using Selective Laser Melting (SLM), and its mechanical behavior was evaluated through tensile testing alongside detailed microstructural investigations. Advanced characterization techniques including Electron Backscatter Diffraction (EBSD), Electron Channeling Contrast Imaging (ECCI), and Digital Image Correlation (DIC) were employed to analyze the relationship between microstructural features and damage evolution in the SLM-fabricated Ti–6Al–4V alloy. Jia Y.F. et al. [14] highlighted the increasing adoption of Ti–6Al–4V in aerospace applications and noted the suitability of SLM as an additive manufacturing process due to its ability to produce intricate geometries with high dimensional accuracy and surface finish. However, the study pointed out that the as-built SLM components exhibited limited ductility and poor fatigue crack growth (FCG) performance, primarily due to the presence of martensitic microstructure and residual stresses. Heat treatment & hot isostatic pressing improved the strength of fractures and FCG resistance, while surface machining showed little effect. Fu R. et al. [15] explored the potential of vegetable oils as environmentally sustainable alternatives to conventional petroleum-based lubricants. While their biodegradability and renewability are advantageous, their inherent lack of anti-wear performance limits widespread industrial use. The study examined the worn surface morphology and tribofilm formation using Field-Emission Scanning Electron Microscopy (FESEM) and Energy-Dispersive Spectroscopy (EDS). Additionally, the corrosive behaviour of oil blends was assessed through copper strip corrosion testing following ASTM D130 standards. Lubrication (SQL) that results in the reduction of cutting temperature as well as tool wear. Ling C et al. [16] investigated and came to a conclusion that using nano earth particles with lubricating oil could boost up the tribological performance and quality of surface can be increased. Yu AH et at. [17] noticed that the nanoparticles can increase its lubricant properties when added in the conventional coolant. The small size of nano particles reduces the friction force and promotes lubrication properties. The lubrication using nano fluids results in decrease in friction and the temperature decrease at the tool tip that helps to maintain the tool hardness and tool cutting edge sharpness is also maintained.

This paper discussed about the machining of Ti-fiAl-4V with different modes of lubrication. Here we use dry lubricant, conventional fluid, plain rubber seed oil, nano additives added rubber seed oil. The cutting force, cutting temperature and surface roughness are calculated and inspected.

2. METHODOLOGY

2.1 Experimental Procedure

A cylindrical titanium alloy rod with a diameter of 25 mm and a length of 300 mm was employed as the workpiece material. The chemical composition and mechanical properties of the Ti-6Al-4V alloy are detailed in Table 1 and Table 2, respectively. Tungsten carbide tools, fabricated through powder metallurgy and composed of a hard carbide phase bonded by a softer metallic matrix, were utilized for the machining trials. Initial spectrometric analysis and turning operations were performed using a cutting fluid derived from vegetable oil. This fluid forms a stable milky emulsion when mixed with water and incorporates rust inhibitors to enhance its anti-corrosive performance. Based on the machining

parameters outlined in Table 3, a total of 16 experimental runs were conducted. The cutting fluid was applied intermittently in a dropwise manner during the machining process through a controlled delivery system. Figures 1(a) and 1(b) illustrate the lathe tool dynamometer setup and the machining operation, respectively.

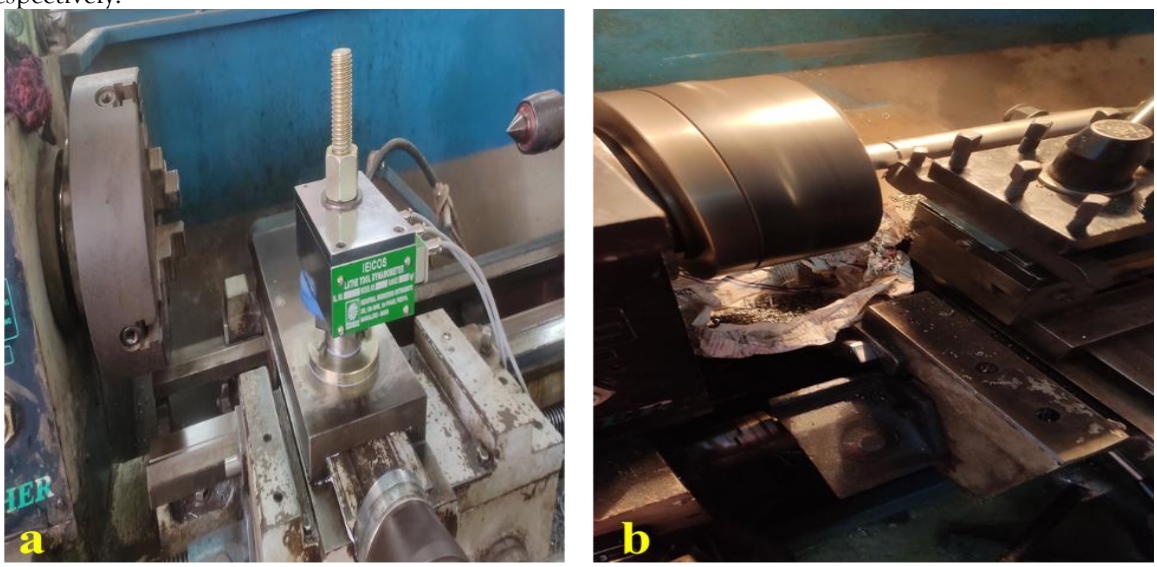

Fig. 1 a) Tool lathe dynamometer b) Machining process

Table 1. Ti-6Al-4V - Chemical Composition of [18,19]

Ti	Al	V	Fe	O	C	N	H
89.364	6.18	4.12	0.12	0.17	0.03	0.01	0.0053

Table 2. Ti-6Al-4V - Mechanical Properties [18,19]

Hardness (HV)	347
Melting point (^{0}C)	1661
Ultimate tensile strength (MPa)	631
Yield strength (MPa)	744
Impact toughness (J)	33
Elastic modulus (GPa)	112
Density (g/cm^2)	4.51
Thermal conductivity at 20^{0}C (W/mK)	6.61
Elongation (%)	8

Table 3. Cutting parameters

Cutting speed (rn/min)	40/80/120/160
Feed (mm/rev)	0.1/0.2/0.3/0.4
Depth of cut (mm)	0.2/0.4/0.6/0.8
Types of lubrication	Water soluble liquid, esterified & improved RSO

2.2. Coolant Preparation

Rubber seed oil (RSO) was extracted through mechanical pressing of rubber seeds. To lower the acid value of the crude oil, an esterification process was carried out. This acids-catalyzed esterification reduces the free fatty acid (FFA) content by reacting oil triglycerides and methanol in with the help of a catalyst containing acids. In this study, sulphuric acid (H_2SO_4) was utilized as the catalyst.

Initially, 200 mL of RSO was heated to 60 °C in a 500 mL conical flask and subsequently allowed to cool. Following this, 100 mL of methanol (equivalent to 50% v/v of the oil) was added and the mixture was stirred. After a few minutes of stirring, sulphuric acid (1% v/v) was introduced into the mixture. The esterification reaction was maintained for 1 hour at a constant temperature of 45 °C under continuous

stirring. Upon the reaction was complete, the resultant mixture was placed in a separating funnel and left to settle for 8 hours. The denser aqueous phase, containing methanol, water, and sulphuric acid, separated and settled at the bottom, along with a layer of residue composed of pigments, waxes, and gum-forming substances.

A second esterification step was conducted using a methanol-to-oil ratio of 80% v/v and 2% v/v H_2SO_4, while maintaining the same reaction conditions. This two-step process, with a total reaction time of 2 hours at 45 °C, yielded the most favourable results. Post-reaction, the residue and aqueous methanol layer were separated, and the acid value of the esterified RSO was determined using the standard AOCS (American Oil Chemists' Society) method.

Subsequently, the esterified RSO was enhanced by incorporating 3% (by volume) of molybdenum disulphide (MoS_2) nanoparticles. MoS_2 was selected due to its low friction coefficient, excellent thermal and chemical stability, high catalytic activity, and favorable tribological properties. Figures 2(a), 2(b), and 2(c) illustrate the stages of plain RSO, RSO during settling, and fully settled RSO, respectively [20,21].

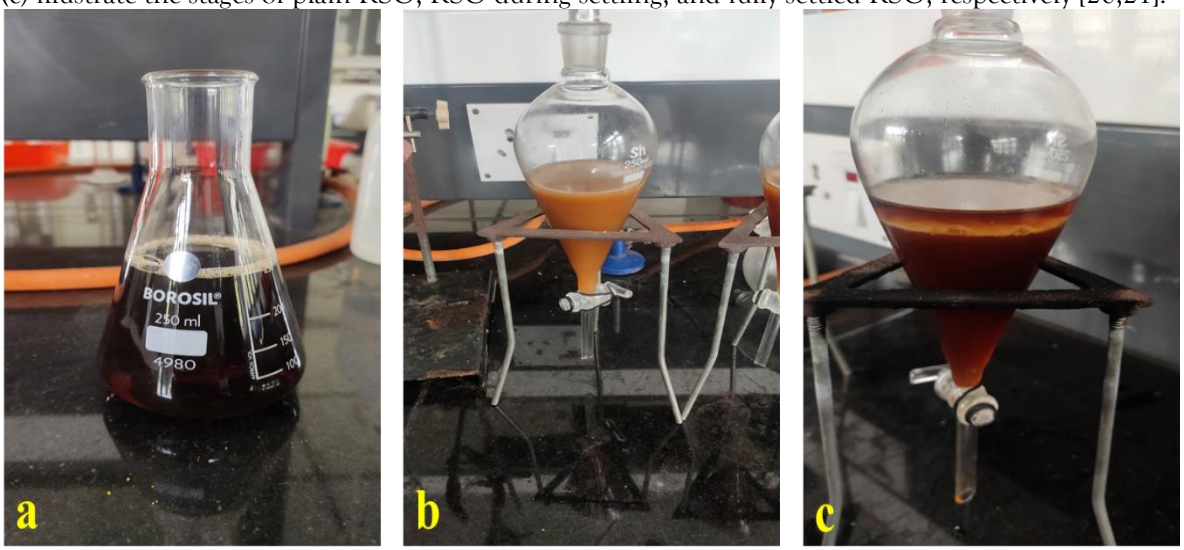

Fig. 2 a) Plain RSO, b) Settling RSO c) Settled RSO

3. RESULTS AND DISCUSSION

A total of 36 machining experiments were conducted. The workpiece was evaluated both during and after the machining process. For each of these 36 trials, measurements were recorded for cutting force, tool tip temperature, and surface roughness. The experimental results were systematically organized according to the lubrication condition employed. Tables 4, 5 and 6 present the detailed outcomes corresponding to each lubricant type tested.

Table 4. Test results with Water Soluble Cutting Fluid

Sl.No	Mode of Lubrication	Speed (rpm)	Depth of Cut (mm)	Cutting Force (N)	Surface Roughness (µm)	Temperature (°C)
1	Water Soluble Liquid	45	0.5	376	0.724	38.3
2	Water Soluble Liquid	45	1	332	0.843	38.4
3	Water Soluble Liquid	45	1.5	330	0.856	37.4
4	Water Soluble Liquid	60	0.5	292	2.241	36.8
5	Water	60	1	326	1.764	37.4

	Soluble Liquid Water					
6	Soluble Liquid Water	60	1.5	335	1.475	37.4
7	Soluble Liquid Water	90	0.5	248	2.148	38.6
8	Soluble Liquid Water	90	1	305	2.062	37.1
9	Soluble Liquid Water	90	1.5	318	1.948	41
10	Soluble Liquid Water	145	0.5	272	1.013	37.7
11	Soluble Liquid Water	145	1	324	0.947	43.4
12	Soluble Liquid	145	1.5	357	0.79	38.2

Table 5. Test results with Esterified Rubber Seed Oil as Cutting Fluid

Sl.No	Mode of Lubrication	Speed (rpm)	Depth of Cut (mm)	Cutting Force (N)	Surface Roughness (µm)	Temperature (°C)
1	Esterified RSO	45	0.5	252	2.431	36.5
2	Esterified RSO	45	1	308	1.451	36.8
3	Esterified RSO	45	1.5	314	1.224	37.1
4	Esterified RSO	60	0.5	154	2.308	37.2
5	Esterified RSO	60	1	142	2.165	37.5
6	Esterified RSO	60	1.5	236	2.22	37.6
7	Esterified RSO	90	0.5	165	1.872	35.9
8	Esterified RSO	90	1	220	1.887	36.4
9	Esterified RSO	90	1.5	300	1.797	36.8
10	Esterified RSO	145	0.5	146	0.92	36.7
11	Esterified RSO	145	1	217	0.765	37.2
12	Esterified RSO	145	1.5	279	0.644	35.9

Table 6. Test results with MoS_2 added Rubber Seed Oil as Cutting Fluid

Sl.No	Mode of	Speed	Depth of	Cutting	Surface	Temperature

	Lubrication	(rpm)	Cut (mm)	Force (N)	Roughness (μm)	(°C)
1	Improved RSO	45	0.5	184	0.658	31.8
2	Improved RSO	45	1	276	0.694	32.4
3	Improved RSO	45	1.5	292	0.86	32.6
4	Improved RSO	60	0.5	120	1.843	33.4
5	Improved RSO	60	1	106	1.968	33.6
6	Improved RSO	60	1.5	196	1.884	34.1
7	Improved RSO	90	0.5	102	1.242	31.6
8	Improved RSO	90	1	182	1.354	32.2
9	Improved RSO	90	1.5	262	1.368	32.4
10	Improved RSO	145	0.5	108	0.523	31.3
11	Improved RSO	145	1	148	0.582	31.8
12	Improved RSO	145	1.5	186	0.492	12

3.1. Cutting Temperature

The incorporation of MoS_2 nanoparticles into rubber seed oil (RSO) transforms the base fluid into a nanofluid, significantly modifying its thermophysical properties. The enhanced heat transfer capability imparted by the nanoparticles plays a critical role in improving the cooling efficiency during machining operations. Elevated cutting temperatures typically accelerate tool wear and contribute to dimensional inaccuracies on the machined surface [22].

Experimental investigations conducted under varying cutting conditions reveal that the MoS_2-based nanofluids offer superior thermal performance. The cutting temperature at the tool–workpiece interface exhibited a consistent downward trend in the following order: dry cutting, conventional cutting fluid, plain RSO, and MoS_2-enhanced RSO. As expected, higher cutting speeds led to increased temperatures at the chip–tool interface. However, with increasing concentrations of MoS_2 in the nanofluid, the cutting temperature showed a marked reduction, attributed to the improved thermal conductivity and lubrication effect.

The nanoparticles form a durable, adherent lubricating film on the metal surfaces, minimizing friction and thermal load. Additionally, applying the coolant under higher pressure further enhances its effectiveness by improving penetration to the tool tip and tool–chip interface, ensuring optimal lubrication and heat dissipation [23]. In contrast, chip entrapment in this region can elevate frictional forces, thereby increasing cutting temperature. Figure 3 illustrates the connection between temperature and time under different cooling conditions.

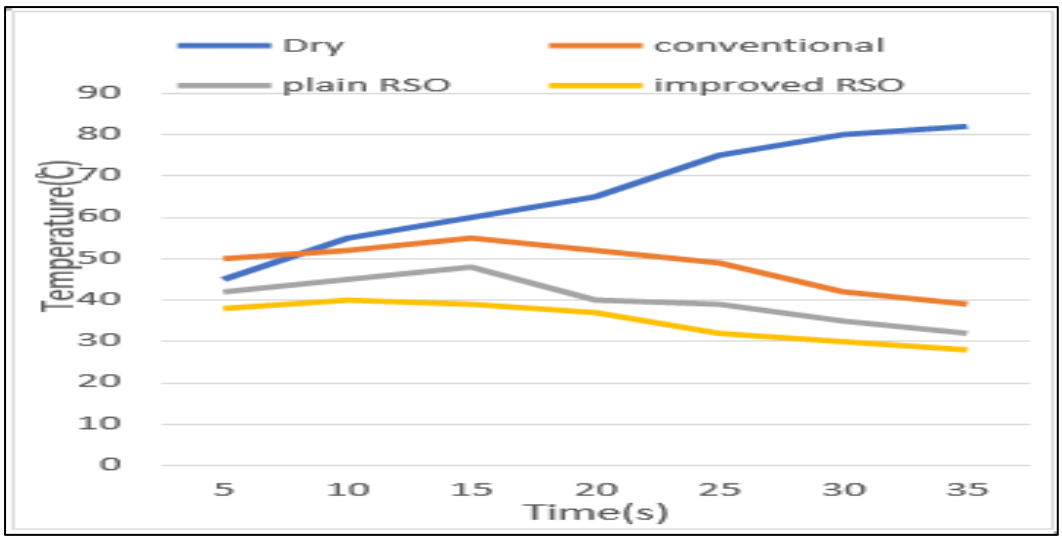

Fig. 3 Variation between temperature and time

3.2 Wear Analysis

Surface quality can be measured using surface evaluation tests. However, the entire quality cannot be measured by using existing traditional tests. So in order to analyse the surface roughness of our work piece Ti-6Al-4V, surface roughness test is used with the different modes of lubrication as shown in figure 4.

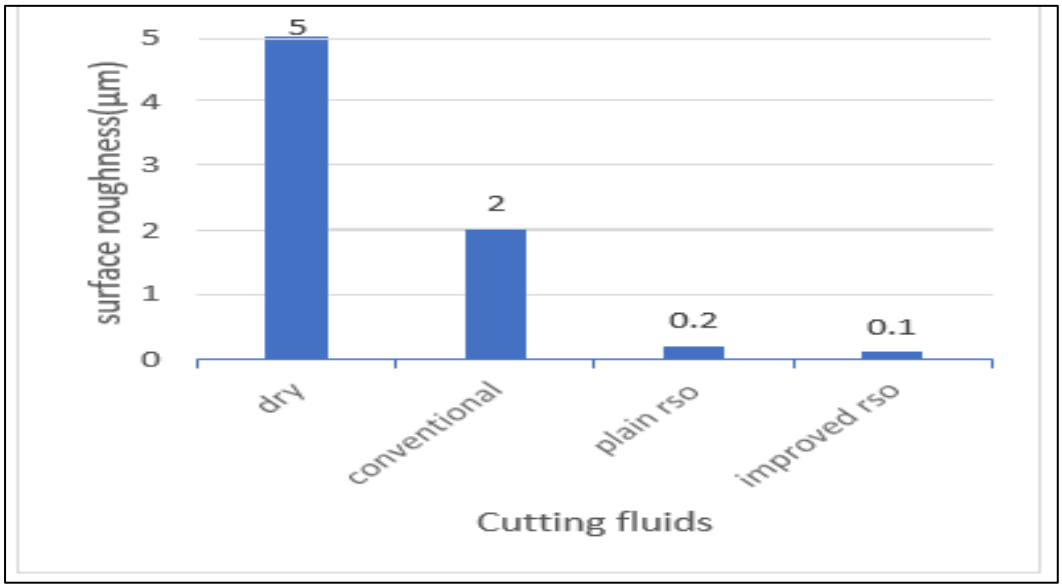

Fig. 4 Mode of lubrication vs Surface Roughness

The surface roughness values of any work piece will change in accordance with the changes that are happening in the cutting speed [24]. By the application of rubber seed oil instead of all other conventional oil surface roughness and cutting temperature values can be reduced. This values will furthermore reduce by the application of nano additives such as molybdenum disulphide in RSO. Mitutoyo portable surface roughness testers measured roughness. The instrument has a 17.5 mm range along the X-axis and up to 360 µm along the Y-axis, enabling precise evaluation of surface texture.

3.3 Tool Tip Temperature

The MoS2 were added to the esterified RSO which showed an improved results com- pared to the conventional fluid and the esterified RSO. The temperature reduced by a great amount from conventional to improved RSO. Figure 5 shows the variation of cutting temperature under different speeds and depth of cut for the types of lubrication. The cutting temperature at the tool–workpiece interface exhibited a decreasing trend from conventional cutting fluid to esterified rubber seed oil (RSO), with the lowest temperature recorded when using the improved RSO formulation. This is due to the additive properties of MoS2 which reduced the heating at cut- ting zone and thus helped to reduce the tool tip temperature and increased the thermal conductivity. No traces of Built Up Edge (BUE) was found

when the microscopic analysis of improved RSO machined work piece was tested and compared with the conventional fluid machined work piece [25]. This showed that the RSO can be used as a cutting fluid while machining and adding additives according to the properties to be achieved can be varied and will improve the machining properties of the material.

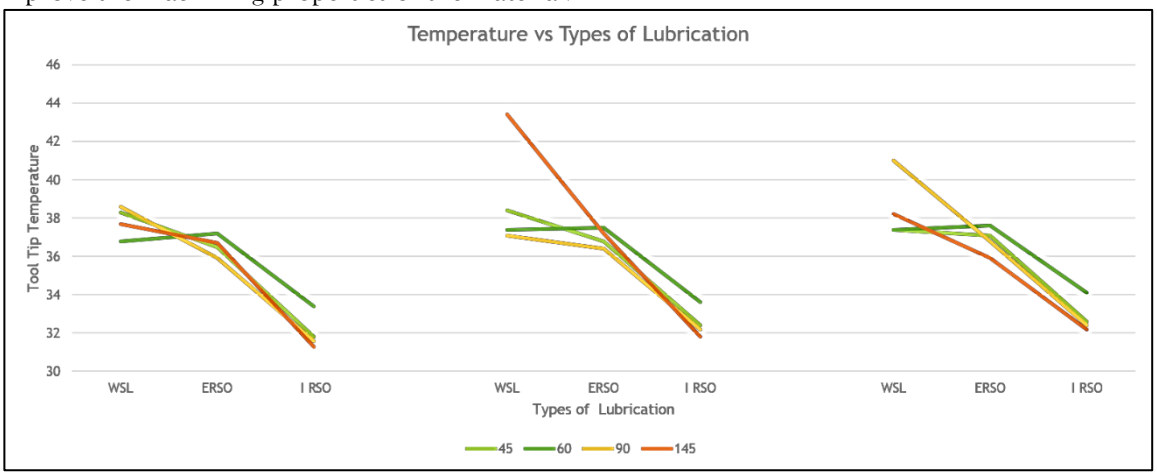

Fig. 5 Temperature vs Lubrication

3.4 Cutting Force at various depths of cut

The experimental findings clearly demonstrate that the cutting force experienced during the machining of Ti-6Al-4V titanium alloy rods decreased as the lubrication method was varied. Moreover, it was observed that cutting force diminished progressively with an increase in cutting speed, with higher forces recorded at lower speeds, consistent with the typical behaviour observed in machining titanium alloys [25].The cutting force variation with speed will be in the order Dry > Conventional > Plain RSO > Improved RSO. Figure 6 shows the graph between cutting force v/s cutting speed.

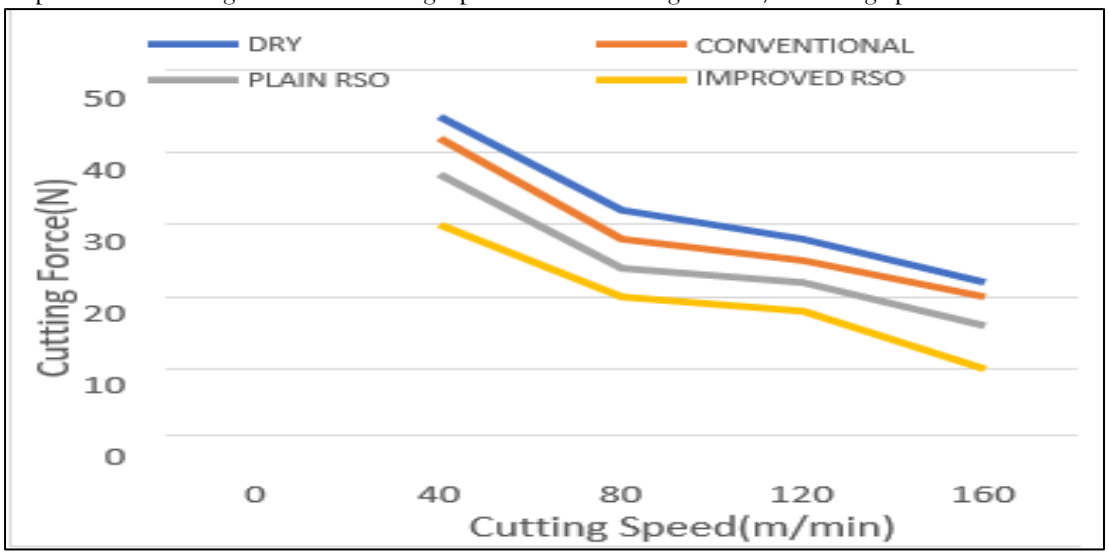

Fig. 6 Cutting force vs Cutting Speed

Figure 7 presents the relationship between cutting force and cutting speed measured across different depths of cut for various cutting fluids. Notably, the most favourable outcomes were achieved at a cutting depth of 1 mm and a spindle speed of 145 rpm. Under these conditions, the enhanced rubber seed oil (RSO) formulation resulted in significantly lower cutting forces compared to both the conventional water-soluble fluid and the esterified RSO. The descending order of cutting force reduction among the lubricants tested was as follows: improved RSO, esterified RSO, and water-soluble lubricant. The cutting force decreases in the order: Conventional Fluid >Esterified RSO>Improved RSO.

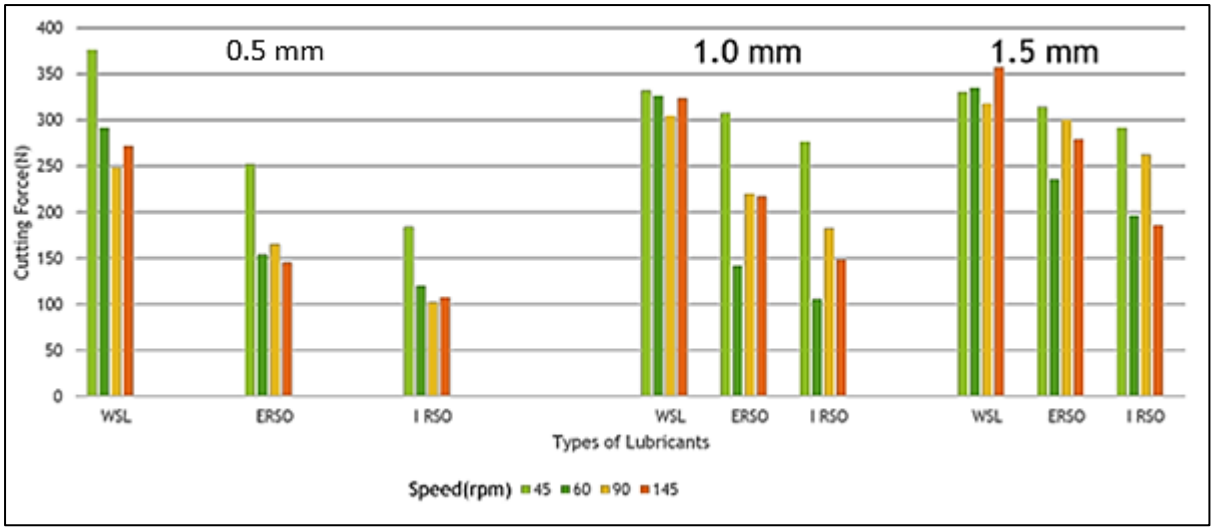

Fig 7. Cutting Force variation at various speeds and depth of cut for varying cutting fluids

4. CONCLUSION

The present investigation demonstrates that the use of biodegradable nanofluids formulated by dispersing MoS_2 nanoparticles into esterified rubber seed oil can significantly enhance the machinability of Ti-6Al-4V alloy during turning operations. The application of these nanofluids resulted in a marked reduction in cutting temperatures at the tool–workpiece interface, indicating improved thermal management compared to conventional cutting fluids. Substantial decreases in cutting forces were also observed, contributing to lower mechanical stresses on the cutting tool and improved process stability. The experimental results further revealed a notable suppression of built-up edge formation, which is a critical factor affecting tool life and surface integrity. Additionally, the incorporation of nano-additives MoS_2 led to a significant improvement in surface finish quality, as evidenced by reduced surface roughness values across all tested conditions. Overall, the study establishes that esterified biodegradable cutting fluids, particularly when tailored with functional nano-additives, present a promising sustainable alternative to conventional lubricants for machining titanium alloys. The findings highlight the potential for customizing such formulations to target specific performance objectives, including thermal regulation, friction reduction, and surface quality enhancement. This work contributes to the growing body of research supporting the integration of environmentally benign lubricants into advanced manufacturing processes, thereby promoting both operational efficiency and ecological sustainability.

Acknowledgments

Authors are thankful to Department of Mechanical Engineering, Saintgits College of Engineering (Autonomous), Kottayam, Kerala, India, for providing platform for this research.

Authors' contributions

C.P and RAK: conceptualization, methodology, investigation, formal analysis, writing – review & editing, and supervision; SMC: data collection, investigation, and writing – original draft. All authors reviewed the manuscript.

Availability of data and materials

Data available within the article.

Funding

The authors received no funding for this work.

Declarations

Conflict of interest:

The authors declare that they have no conflict of interest.

REFERENCES

1. Akbari P, Zamani M, Mostafaei A. Machine learning prediction of mechanical properties in metal additive manufacturing. Addit Manuf 2024;91:104320. https:// doi.org/10.1016/j.addma.2024.104320.
2. Wang H, Gao SL, Wang BT, Ma YT, Guo ZJ, Zhang K, et al. Recent advances in machine learning-assisted fatigue life prediction of additive manufactured metallic materials: a review. J Mater Sci Technol 2024;198:111–36. https://doi.org/10.1016/j.jmst.2024.01
3. Shi T, Sun JY, Li JH, Qian GA, Hong YS. Machine learning based very-high-cycle fatigue life prediction of AlSi10Mg alloy fabricated by selective laser melting. Int J Fatigue 2023;171:107585. https://doi.org/10.1016/j.ijfatigue.2023.107585.

4. Sun L, Zhang XC, Wang RZ, Wang XW, Tu ST, Suzuki K, et al. Evaluation of fatigue and creep-fatigue damage levels on the basis of engineering damage mechanics approach. Int J Fatigue 2023;166:107277. https://doi.org/10.1016/j.ijfatigue.2022.107277.
5. Sun GZ, Zheng JW, Zhao ZH. Gas pore-based fatigue strength and fatigue life prediction models of laser additive manufactured Ti-6Al-4V alloy in very high cycle fatigue regime. Mat Sci Eng A 2025;922:147640. https://doi.org/10.1016/j.msea.2024.147640.
6. Cao YH, Chen CY, Xu SZ, Zhao RX, Guo K, Hu T, et al. Machine learning assisted prediction and optimization of mechanical properties for laser powder bed fusion of Ti6Al4V alloy. Addit Manuf 2024;91:104341. https://doi.org/10.1016/j.addma.2024.104341.
7. Li D, Zhang X, Qin R, Xu J, Yue D, Chen B. Influence of processing parameters on AlSi10Mg lattice structure during selective laser melting: manufacturing defects, thermal behavior and compression properties. Opt Laser Technol 2023;161:109182. https://doi.org/10.1016/j.optlastec.2023.109182.
8. Paul, C., Cherian, S. M., Koshy, C. P., Kurien, R. A., & Philip, J. T. (2023). Comparison on Microstructural Evolution and Wear Behavior of Cu–10Sn–XNi Alloy Composite Developed Through GTA Surface Alloying and Friction Stir Processing. Transactions of the Indian Institute of Metals, 76(9), 2549-2555. https://doi.org/10.1007/s12666-023-02992-4
9. Jordan MI, Mitchell TM. Machine learning: trends, perspectives, and prospects. Science 2015;349:255–60. https://doi.org/10.1126/science.aaa8415.
10. Salvati E, Tognan A, Laurenti L, Pelegatti M, Bona FD. A defect-based physicsinformed machine learning framework for fatigue finite life prediction in additive manufacturing. Mater Des 2022;222:111089. https://doi.org/10.1016/j.matdes.2022.111089.
11. Wang HJ, Li B, Xuan FZ. Fatigue-life prediction of additively manufactured metals by continuous damage mechanics (CDM)-informed machine learning with sensitive features. Int J Fatigue 2022;164:107147. https://doi.org/10.1016/j.ijfatigue.2022.107147.
12. Chen J, Liu YM. Fatigue property prediction of additively manufactured Ti-6Al-4V using probabilistic physics-guided learning. Addit Manuf 2021;39:101876. https:// doi.org/10.1016/j.addma.2021.101876.
13. Zhan ZX, Hu WP, Meng QC. Data-driven fatigue life prediction in additive manufactured titanium alloy: a damage mechanics based machine learning framework. Eng Fract Mech 2021;252:107850. https://doi.org/10.1016/j.engfracmech.2021.107850.
14. Jia YF, Fu R, Ling C, Shen Z, Zheng L, Zhong Z, et al. Fatigue life prediction based on a deep learning method for Ti-6Al-4V fabricated by laser powder bed fusion up to very-high-cycle fatigue regime. Int J Fatigue 2023;172:107645. https://doi.org/10.1016/j.ijfatigue.2023.107645
15. Fu R, Zheng L, Ling C, Zhong Z, Hong YS. An experimental investigation of fatigue performance and crack initiation characteristics for an SLMed Ti-6Al-4V under different stress ratios up to very-high-cycle regime. Int J Fatigue 2022;164:107119. https://doi.org/10.1016/j.ijfatigue.2022.107119.
16. Ling C, Jia YF, Fu R, Zheng L, Zhong Z, Hong YS. Fatigue life prediction for LPBFfabricated Ti-6Al-4V up to very-high-cycle regime based on continuum damage mechanics incorporating effect of defects. Int J Fatigue 2024;181:108131. https://doi.org/10.1016/j.ijfatigue.2023.108131.
17. Yu AH, Pan Y, Yue LS, Kuang F, Zhang JZ, Lu X. Explainable machine learning for hardness prediction of laser powder bed fused Ti-6Al-4V and assisting in understanding effects of process parameters. J Alloy Compd 2024;1008:176566. https://doi.org/10.1016/j.jallcom.2024.176566.
18. Semenova, I., Polyakov, A., Gareev, A., Makarov, V., Kazakov, I., & Pesin, M. (2023). Machinability Features of Ti-6Al-4V Alloy with Ultrafine-Grained Structure. Metals, 13(10), 1721. https://doi.org/10.3390/met13101721
19. Goettgens, V. S., Weber, L., Braun, J., Kaserer, L., Letofsky-Papst, I., Mitsche, S., ... & Leichtfried, G. (2024). Microstructure and Mechanical Properties of Ti-6Al-4V In Situ Alloyed with 3 wt% Cr by Laser Powder Bed Fusion. Metals, 14(6), 715. https://doi.org/10.3390/met14060715
20. Du LM, Qian G, Zheng L, Hong YS. Influence of processing parameters of selective laser melting on high-cycle and very-high-cycle fatigue behaviour of Ti-6Al-4V. Fatigue Fract Eng Mater Struct 2021;44:240–56. https://doi.org/10.1111/ ffe.13361.
21. Du LM, Pan XN, Qian GA, Zheng L, Hong YS. Crack initiation mechanisms under two stress ratios up to very-high-cycle fatigue regime for a selective laser melted Ti6Al-4V. Int J Fatigue 2021;149:106294. https://doi.org/10.1016/j.ijfatigue.2021.106294.
22. Liu FL, He C, Chen Y, Zhang H, Wang QY, Liu YJ. Effects of defects on tensile and fatigue behaviors of selective laser melted titanium alloy in very high cycle regime. Int J Fatigue 2020;140:105795. https://doi.org/10.1016/j.ijfatigue.2020.105795.
23. Brot G, Koutiri I, Bonnand V, Favier V, Dupuy C, Ranc N, et al. Microstructure and defect sensitivities in the very high-cycle fatigue response of Laser Powder Bed Fused Ti-6Al-4V. Int J Fatigue 2023;174:107710. https://doi.org/10.1016/j.ijfatigue.2023.107710.
24. Fu R, Zheng L, Zhong Z, Hong YS. High-cycle and very-high-cycle fatigue behavior at two stress ratios of Ti-6Al-4V manufactured via laser powder bed fusion with different surface states. Fatigue Fract Eng Mater Struct 2023;46:2348–63. https://doi.org/10.1111/ffe.13985.
25. Jin P, Tang Q, Li K, Feng QX, Ren ZH, Song J, et al. The relationship between the macro- and microstructure and the mechanical properties of selective laser-melted Ti6Al4V samples under low energy inputs: simulation and experimental. Opt Laser Technol 2022;148:107713. https://doi.org/10.1016/j.optlastec.2021.107713.
26.